The Surface Contour Radar, A Unique Remote Sensing Instrument

JAMES E. KENNEY, ENZO A. ULIANA, AND EDWARD J. WALSH, MEMBER, IEEE

Abstract—**A 36-GHz computer-controlled airborne radar has been developed by NRL and NASA WFC which generates a false-color coded elevation map of the sea surface below the aircraft in real-time and can routinely produce ocean directional wave spectra with off-line data processing.**

I. Introduction

UNDER the sponsorship of the NASA Advanced Applications Flight Experiments Program the Naval Research Laboratory (NRL) and the NASA Wallops Flight Center (WFC) have developed an airborne computer-controlled 36-GHz bistatic radar, designed to measure the directional wave spectra of the ocean surface. It produces a real-time topographical map of the surface beneath the aircraft. Fig. 1 shows the basic measurement geometry of the Surface Contour Radar (SCR).

The design of the system necessitated several tradeoffs in system parameters to achieve both high spatial and high range resolution. The transmitted frequency was arrived at by compromising between the inherent high spatial resolution with moderate apertures at 90 GHz and the ease of generating 1-ns pulses below 18 GHz. An electronically scanned phased array was considered for the transmit antenna but was eliminated for three reasons: 1) lack of necessary bandwidth, 2) tendency to vary pointing with frequency, and 3) cost. At 36 GHz a moderate size elliptical mirror (48 cm × 69 cm) could be mechanically scanned sinusoidally at 10 Hz without incurring permanent mechanical problems in the aircraft structure.

The system uses dual frequency carriers that are spaced far enough apart to be decorrelated on the sea surface. The problem of the limited power available at 36 GHz over a 1-GHz bandwidth was circumvented by pulse-compression techniques. The continuous wave (CW) transmitter is biphase modulated by a digitally generated maximal length code sequence. The return signal is autocorrelated by a like sequence with a variable time delay inserted. The code length and clock rate can be varied, providing selectable range resolutions of 0.15, 0.30, 0.61 and 1.52 m. The RF and antenna packages are mounted in a pod under the fuselage of a NASA C-54 aircraft with the signal processing system located in equipment racks inside the aircraft. Fig. 2 is a picture of the pod installation.

Manuscript received May 29, 1979.

J. E. Kenney and E. A. Uliana are with the Naval Research Laboratory, Washington, DC 20375.

E. J. Walsh is with the NASA Wallops Flight Center, Wallops Island, VA 23337.

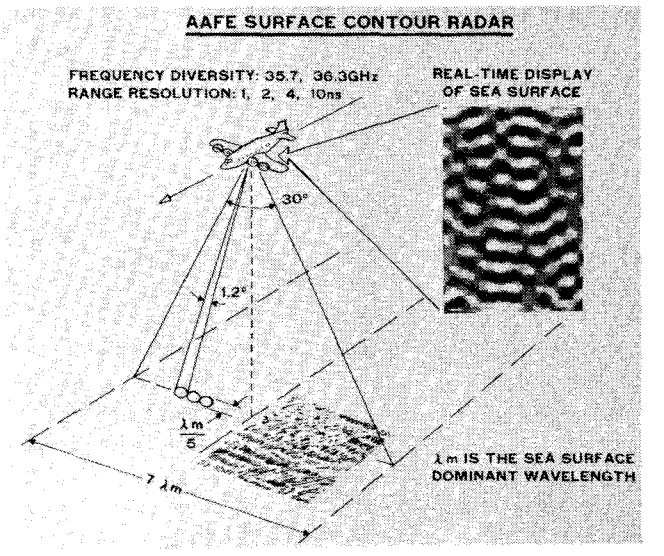

Fig. 1. The basic measurement geometry of the SCR.

II. Antenna System

The transmitting antenna is a horn-fed lens that is directed horizontally to illuminate an elliptical mirror oriented at 45° to the longitudinal axis of the horn-lens system. The mirror reflects the transmitter beam towards the surface beneath the aircraft and is scanned sinusoidally by a motor driven mechanical linkage through approximately a ±16.5° sector with respect to the perpendicular to the aircraft wings. Fig. 3 shows the mirror, its drive housing, the flywheel which is belt driven by a 1/4 hp motor, and the mechanical linkage contained within the drive housing.

Fig. 4 indicates the mirror orientation and the spatial resolution in terms of aircraft altitude h. The half-power beamwidth of the transmitting antenna is 1.2° × 1.2°. The receiving antenna, which is located just to the right of the transmitting antenna, is a lens-corrected compound sectoral horn with a fan beam of 1.2° × 40° at the half-power points. The bistatic antenna system provides a two-way half-power beamwidth of 0.85° × 1.2° for a spatial resolution of approximately $h/70$ by $h/50$ with a swath width of $h/2$. The antenna scan rate is continuously adjustable between 1 and 10 Hz and the antenna position is monitored by a digital shaft encoder of 0.1° resolution.

Since the angular scan is very slow between 15° and 16.5°, where it reverses, data is only acquired while the beam is within approximately ±15°. The angular scan is fixed with respect to the aircraft wings, so the region illuminated by the radar depends on the roll attitude of

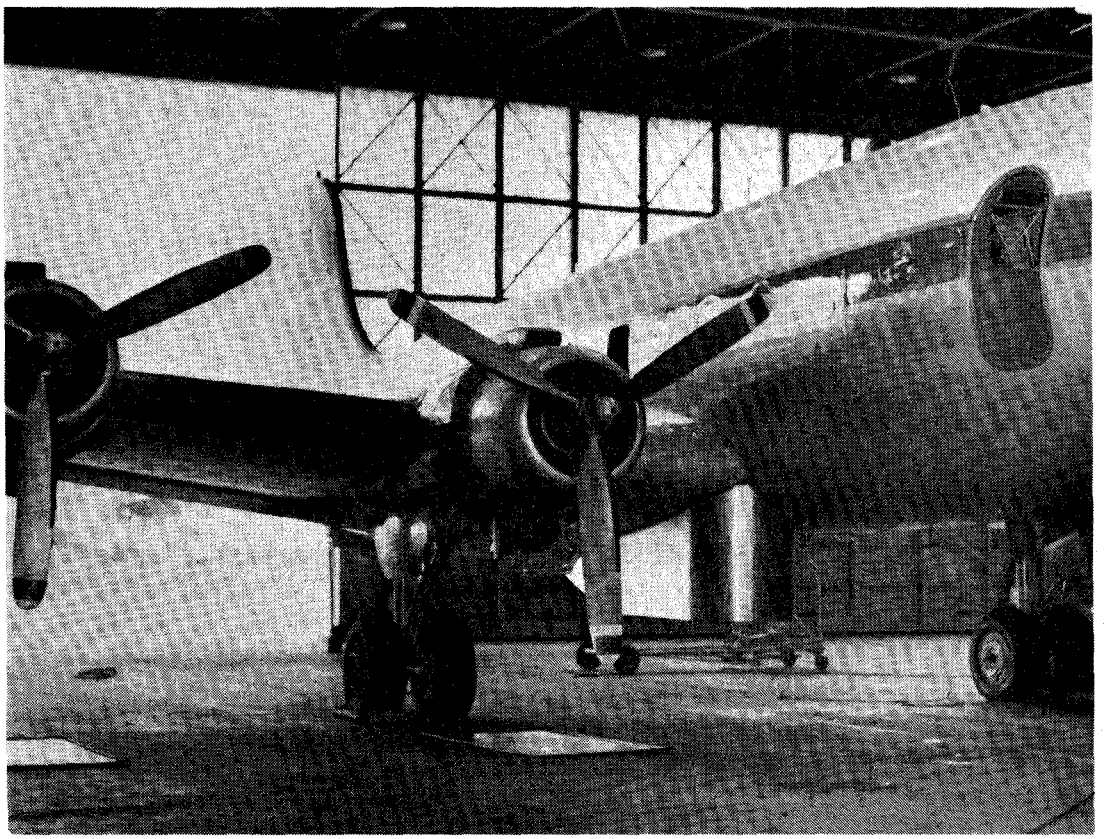

Fig. 2. A pod mounted under the fuselage of a NASA C-54 aircraft contains the SCR RF and antenna packages.

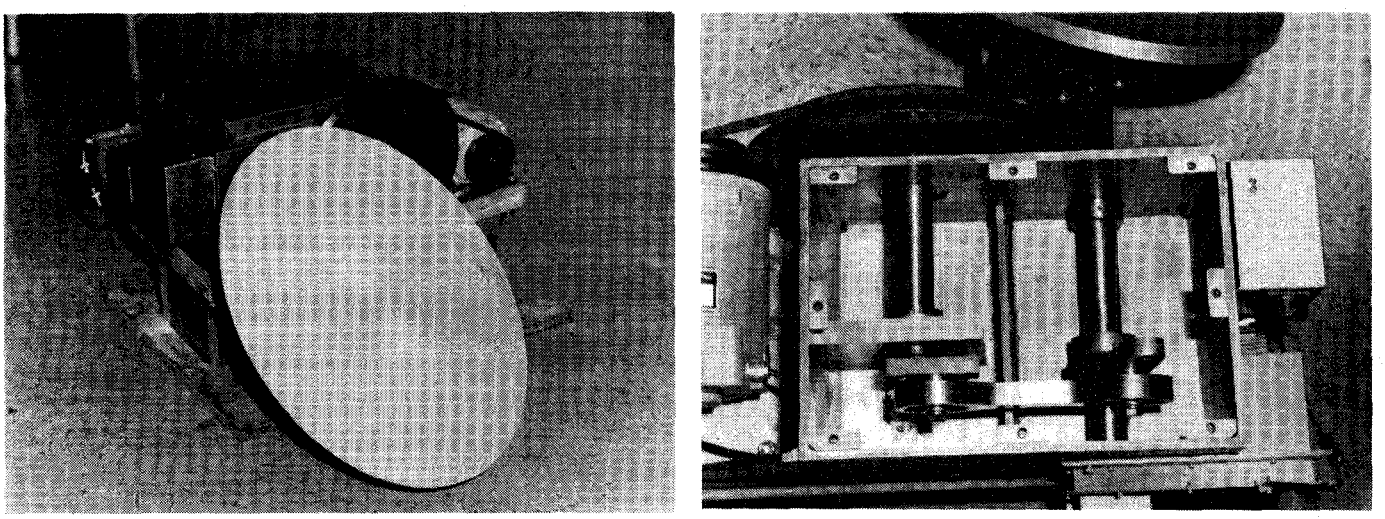

Fig. 3. The oscillating mirror which scans the antenna beam and the mechanical linkage which drives it.

the aircraft. For example, if the aircraft were in a 15° bank to the left, then the radar would interrogate the region to the right of the aircraft ground track.

III. RF Package

Fig. 5 is a block diagram of the transceiver package. It consists of a dual-frequency generator with frequencies located at 35.7 and 36.3 GHz in a master–slave configuration. The difference between the two frequencies is divided down and compared with a 5-MHz standard. The phase comparison loop varactor tunes the slave to maintain it at a constant 600-MHz difference from the master. The two frequencies are power divided with one path of each divider then being combined into a common transmission line which is fed into a modulator. The other two transmission lines are used as local oscillators for the two mixer preamps, generating two 600-MHz receiver IF channels. The IF channels are band limited to 3.5 MHz by a pair of filters and fed to a second IF system via two digitally programmable attenuators (0 to 31 dB in 1-dB increments) that serve as automatic gain control (AGC) adjustments. The second local oscillator is a 570-MHz source that is referenced to the same 5-MHz standard to which the transmitter is compared. The two second IF (30-MHz) channels are then further amplified and passed through 500-kHz filters to square law detectors. The video

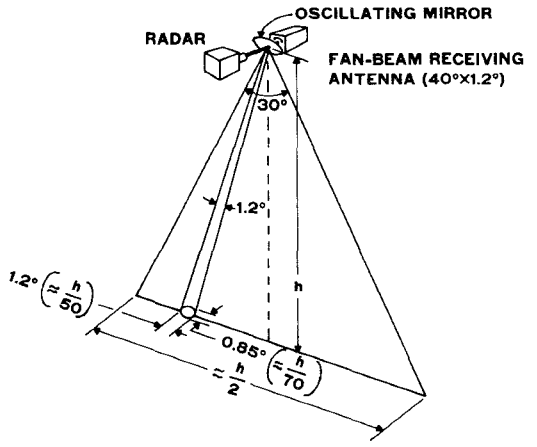

Fig. 4. The antenna and mirror orientation and the spatial resolution in terms of aircraft altitude h.

signals are summed and converted to digital information.

The output of the modulator is routed through a level adjusted attenuator to a waveguide switch which allows the signals to be switched either to the transmitting power amplifier or via a directional coupler into the receiver demodulator. The second signal path is used to determine zero range and will be discussed later. The return signal path is via the receiving antenna and TWT preamplifier to the demodulator and then to the mixer preamps.

IV. Code Generation

The transmitter modulator and receiver demodulator are controlled by two identical code generators that are driven by a common clock which has selectable rates of 100, 250, 500, and 1000 MHz. The code is a pseudo-random maximal length sequence. It is generated digitally by using shift registers with the appropriate feedback connections. The code has a non-repetitive length of $2^n - 1$, where n is the number of shift registers. Fig. 6 is an example of a code sequence employing only three shift registers. The transmitter modulator uses the maximum length sequence to binary phase modulate (0°, 180°) the transmitted sine wave. The receiver demodulator additionally phase modulates the returning signal using the same sequence. Fig. 7 shows examples of the results when the receiver demodulator code is either aligned or misaligned with the phase of the code on the returning signal. If the demodulator maximum length sequence is in phase, the result is an unmodulated sine wave and all the energy in it will pass through the narrow-band post-mixing filter. In all other cases, modulating a maximum length sequence with any phase shifted version of itself will produce the same sequence. Then the narrow-band filter would reject nearly all the energy in the resulting wide-band signal.

The SCR has three code lengths: 2047, 1023, and 511. The 2047 length is used with the 1000-MHz clock rate, the 1023 length with the 500-MHz clock rate, and the 511 length with the 250-MHz clock rate. That results in a roughly constant time interval of 2 μs for each code and an unambiguous range of 305 m for the 0.15, 0.30, and 0.61-m resolutions. The 511 length is used with the 100-MHz clock rate so the time interval and unambiguous range for the 1.52-m resolution are 5 μs and 757 m. The autocorrelation function of the code is shown in Fig. 8 where N is the code length and τ is the period of the clock. The peak sidelobe voltage ratio is N^{-1} [6].

To scan the range being interrogated by the radar, one code is slipped with respect to the other. Suppose the code on the return signal is fortuitously in phase with the receiver demodulator code generator. Then if the clock gate to the receiver code generator were inhibited for one count it would cause the phase of the receiver code to lag one unit relative to the transmitter code. That would mean that the round-trip transit time from the radar to the target would have to increase by one unit for the return signal code to again be in phase with the receiver code generator.

The SCR uses a scan rate generator which is capable of putting out pulses at rates between 1 and 127 kHz, selectable in 1-kHz steps. For the SCR application the PRF is fixed at 90 kHz. A programmable advance-retard signal input to the generators provides a method of inhibiting the clock pulses to either the receiver code (to advance the range interrogated) or the transmitter code (to retard the range interrogated). This allows one of the codes to be slipped with respect to the other and provides a way to scan in range through the return signal to search for code alignment. The SCR can never dwell at a given range. Each 11 μs it moves on to interrogate the adjacent range cell. The only thing that can be controlled is whether the new range is further from or closer to the radar. The clock rate selected for the sequences determines whether the range resolution is 1, 2, 4, or 10 ns.

V. Predetermined Range Scan Patterns

Because many computations were needed to produce a real-time false-color coded topographic map of the region below the aircraft and because the time required to set up a channel to transfer data between the computer and the radar hardware was relatively high, it was decided to limit the transfer of information between hardware and computer to once per lateral sweep of the antenna beam. This

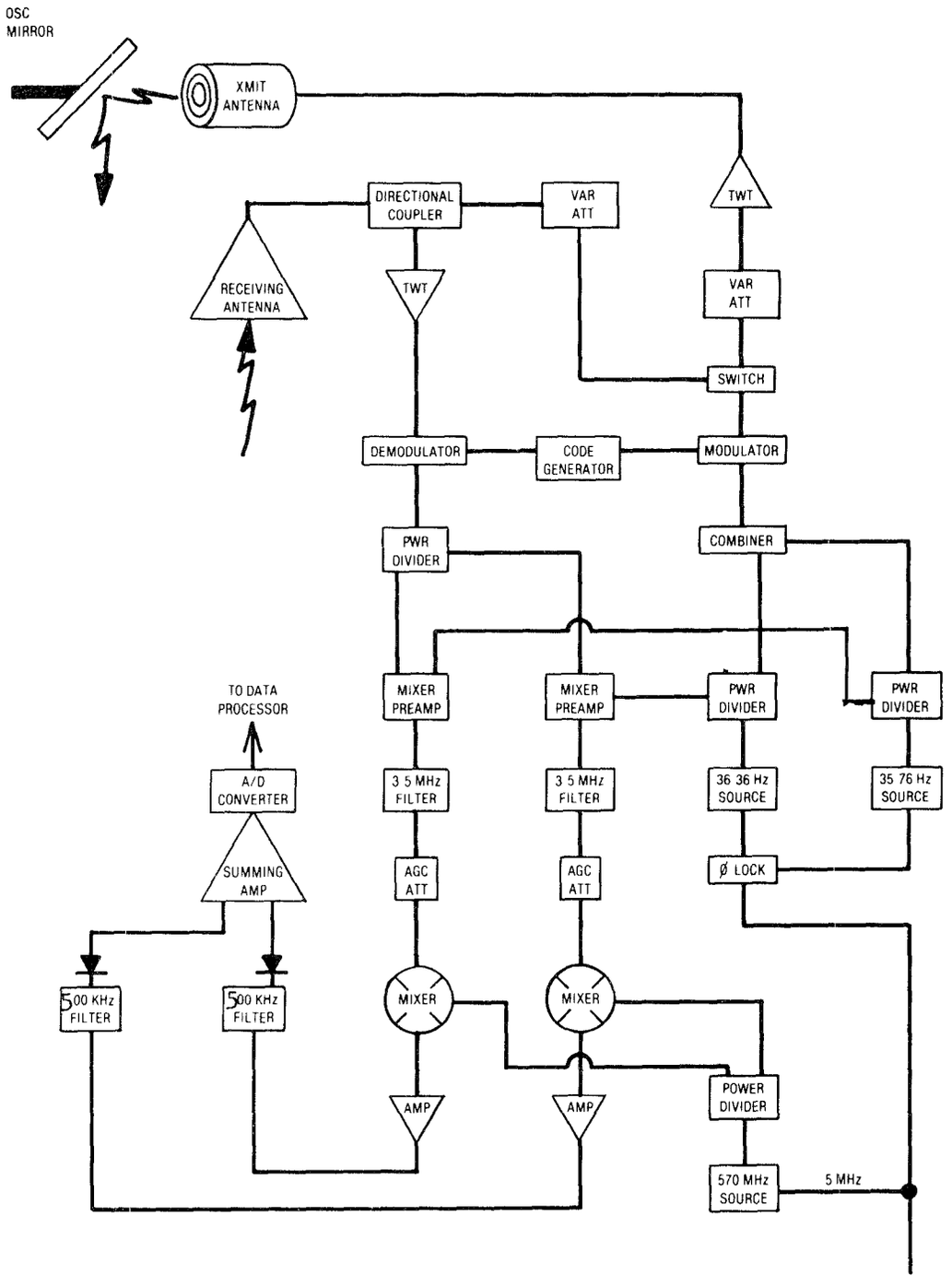

Fig. 5. Block diagram of the transceiver package.

efficiency was achieved by using 51 predetermined sawtooth range scan patterns which would interrogate a vertical region about some horizontal reference level. Three of the 51 range scan patterns for a range resolution of 1 ns, an altitude of 500 m, and a ground speed of 70 m/s are shown in Fig. 9. The first, twenty-sixth, and fifty-first patterns correspond to aircraft roll angles of $-14.7°$, 0°, and 14.7°. The points indicate the position of the center of the antenna beam at the range being interrogated. For the sake of clarity only every other point is shown. Aircraft roll angles exceeding $\pm 14.7°$ are not acknowledged by the system.

The lengths of the segments are calculated with more retard than advance steps when the beam is sweeping towards nadir and vice versa when it is sweeping away from nadir to compensate for the change in the range to the horizontal reference level as a function of incidence angle. The vertical dimension has been magnified by a factor of 20 compared to the horizontal and that has distorted the apparent incidence angles. The incidence angle monotonically approaches the vertical as the nadir point is approached.

To be observed, the surface would have to lie within the range scan pattern. Each of the 51 range scan patterns has

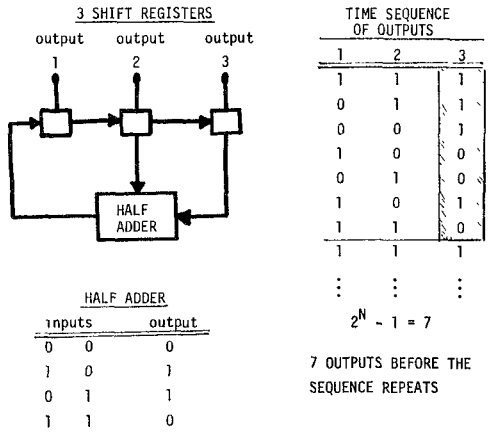

Fig. 6. Example of a pseudo-random maximal length sequence employing only three shift registers.

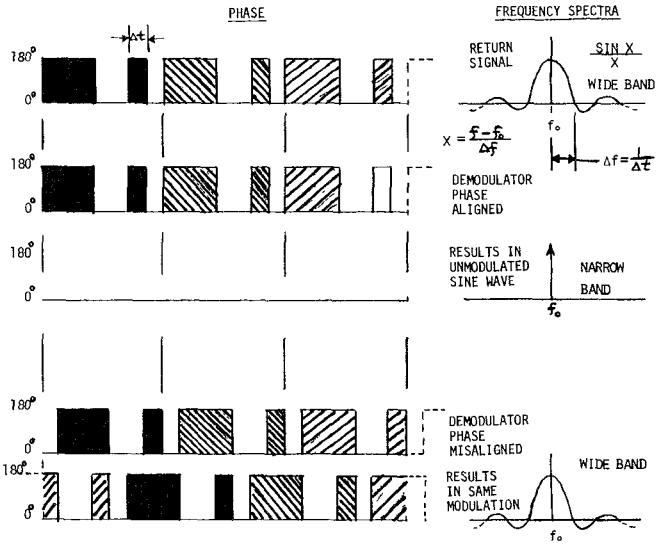

Fig. 7. Examples of what happens when the receiver demodulator code is in phase or out of phase with the code on the returning signal.

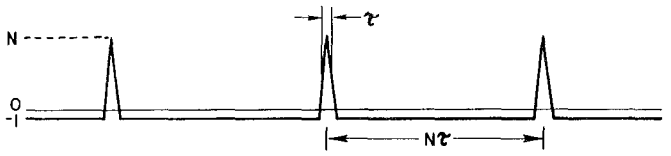

Fig. 8. Autocorrelation function of a maximal length sequence which would result in a peak-sidelobe–voltage ratio of N^{-1}.

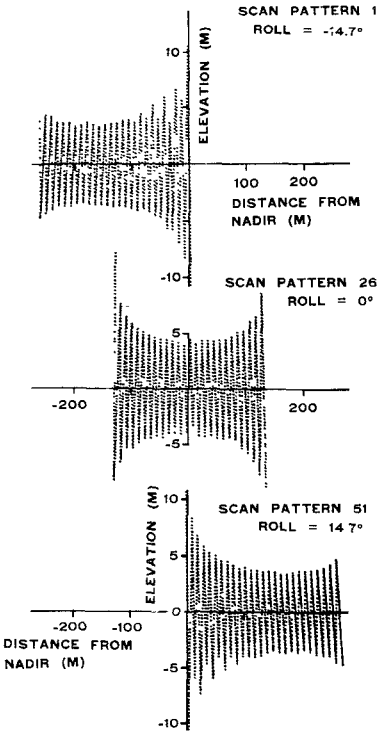

Fig. 9. Three of the 51 predetermined range scan patterns corresponding to a 500-m aircraft altitude, 70 m/s ground speed, and the roll angles indicated. The scan patterns assume an angular scan rate of 9.5 Hz (19 L/s) and that the antenna beam is scanning from right to left. The range resolution is 1 ns and only every other point is shown.

51 legs with each leg occurring during approximately a 0.6° deflection of the antenna beam. The lateral 3-dB two-way beamwidth is 1.2° so the region illuminated moves approximately half a beamwidth from one range scan leg to the next. Each range scan pattern is computed for a particular roll angle such that each of the legs is symmetric about the horizontal reference level of the pattern. When the roll attitude of the aircraft changes by approximately 0.6° the adjacent range scan pattern is used so that the region interrogated remains symmetrical with respect to the horizontal reference level.

The 51 scan patterns are computed assuming that the antenna beam is swinging from right to left. But it is apparent in Fig. 9 that the scan pattern 1 for a roll angle of $-14.7°$ and the beam swinging from right to left could be used for a roll angle of 14.7° if the beam were swinging from left to right. Similarly, scan pattern 51 could be used for either a roll of 14.7° when the beam is swinging from right to left or for a roll of $-14.7°$ when the beam is swinging from left to right.

The scan patterns are designed to determine the elevations at equally spaced intervals on the ground. When the aircraft roll is zero the total included angle of the scan pattern is 30° but when the roll angle is 14.7° it is only 28° because the horizontal distance from nadir is proportional to the tangent of the angle off-nadir.

VI. Steady-State Signal Processing

Range tracking, elevation computation, and system management are accomplished in software using a minicomputer as the central processor. Fig. 10 is a block diagram of system information flow. The quantities recorded on magnetic tape at the end of each antenna scan include: the raw radar data, the computed elevations, the miscellaneous parameters used for housekeeping and to maintain antenna scan and range scan synchronization, the aircraft LTN-51 Inertial Navigation System (INS) information (latitude, longitude, ground speed, ground track, heading, roll), date, and time of day. Nearly all of the real-time computations performed by the computer use integer arithmetic to minimize running time. Quantities of length and time are normalized by Δr, the radar-range resolution, and Δt, the 11-μs range scan rate period, respectively, and dealt with as integers. Scaled integer

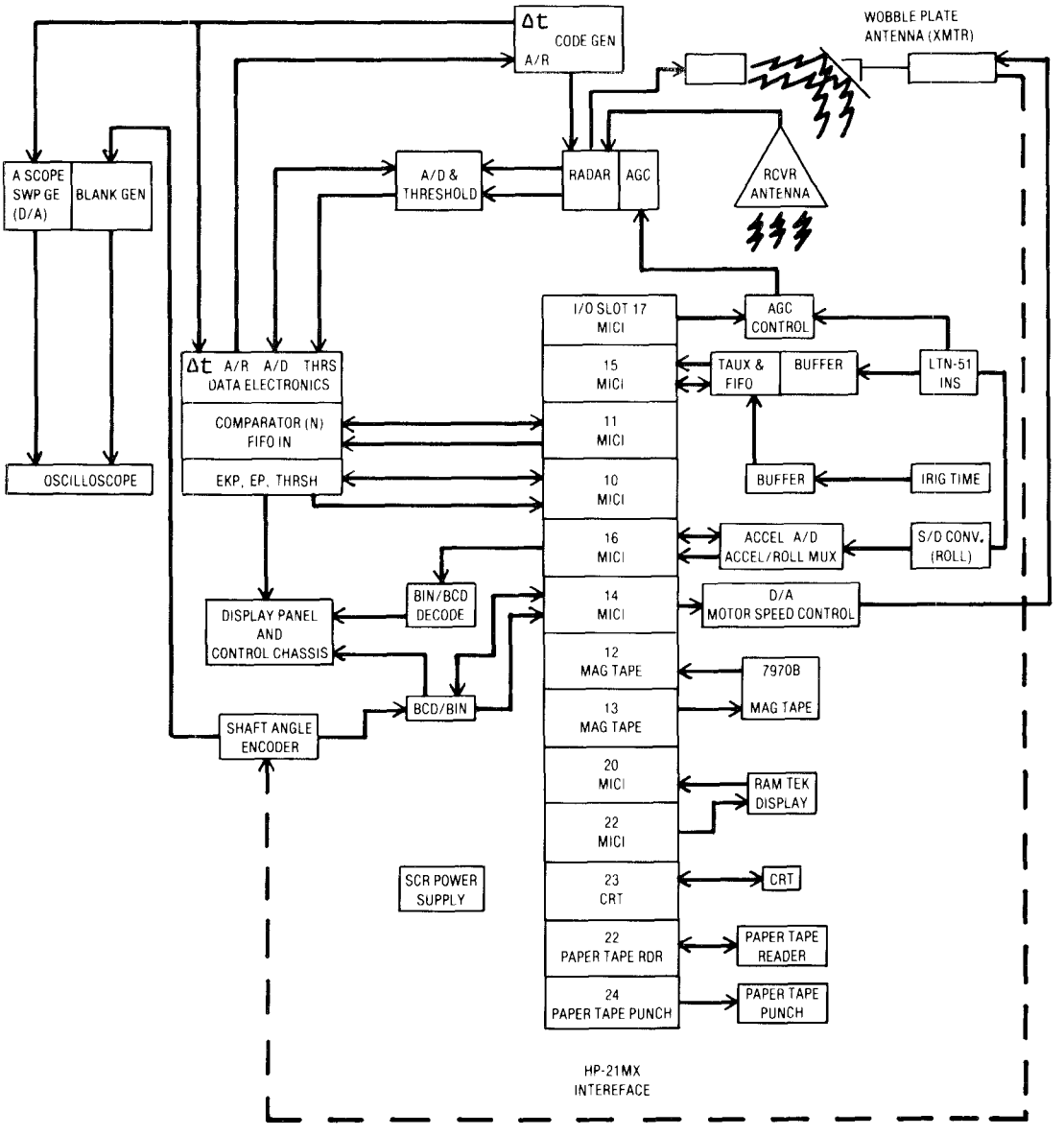

Fig. 10. Block diagram of system information flow.

arithmetic is used wherever necessary to maintain accuracy.

Preprocessing of the return signals by the radar hardware reduces the computational load on the computer and permits the reduction of the interaction between the radar hardware and the computer to once per lateral scan of the antenna beam. The video signal is digitized for each range cell and that value is both accumulated and multiplied by its associated range number referenced to the start of the leg. That product is also summed. At the end of each range scan leg, the sum of the powers from each range (ISP), the sum of the range weighted powers (ISKP), and a number indicating the position on the leg where the return signal first exceeded a fixed threshold are stored in a data memory. The data memory is a first-in first-out (FIFO) device that is 16 bits by 255 bits. Since the computer is a 16-bit machine, ISP and ISKP are divided into two 16-bit words and the threshold count becomes a fifth 16-bit word. During each lateral scan of the antenna beam, data is saved from the 51 range scan legs in the form of five 16-bit words which fill the FIFO. At the end of each lateral scan, the 255 words are transferred into the computer where each ISKP is divided by the associated ISP to determine KBAR, the centroid of power for that leg of the range scan.

Fig. 11 shows a portion of a range scan pattern and indicates the computation of the surface elevation IELEV(N), where N is an index indicating which of the 51 range scan legs is under consideration. When the scan patterns were precomputed during the startup phase, the range to the beginning of each leg IR(N), was stored in the computer, as well as the cosine of the angle of that point from nadir. The range to the centroid of the return power is then found by adding or subtracting KBAR from IR(N). (Range decrements on odd numbered legs and increments on even numbered legs.) The cosine of the angle off-nadir corresponding to the centroid of the return power is found by linearly interpolating between the val-

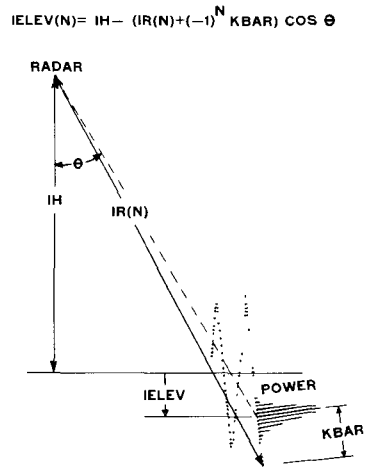

Fig. 11. A portion of a range scan pattern with the computation of surface elevation indicated.

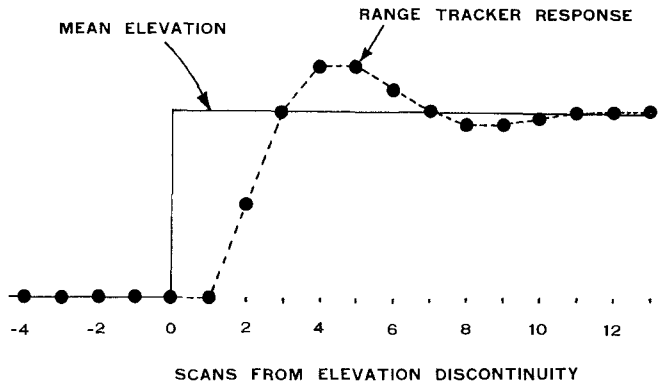

Fig. 12. Range tracker response to a step function in mean elevation.

ues at the end points of the leg using the ratio of KBAR to the total number of steps in that leg. The actual computations employ the cosine complement (1 − cosine) multiplied by 100 000 so that high accuracy may be maintained using integers while keeping the values below the 32 768 computer limit on the magnitude of an integer. The computer multiplies the range by the cosine of the angle to determine the vertical distance to the surface and subtracts that quantity from the nominal aircraft altitude, IH, to determine the surface elevation with respect to the reference level.

Another FIFO which is 12 bits wide by 128 bits deep serves as a range scan memory to hold information to control the radar hardware. A complete range scan pattern has 64 legs but no data is saved from the first 13. They are used to waste time while the oscillating mirror slows down and reverses its direction. The starting elevation for the 51 range scan legs on which the radar data is saved can be shifted up or down by varying the total number of advance versus retard steps in those first 13 legs. By making adjustments in the total number of steps in the time waster legs it is possible to maintain synchronization between the range scan pattern and the angular scan of the beam.

The synchronization adjustment has two components. First, the period of the oscillating mirror is measured on each angular scan and there is an immediate adjustment for any variation from its nominal value. Second, the oscillating mirror shaft angle encoder is sampled at the end of each range scan pattern, compared to the nominal value for that scan pattern, and a partial correction is applied. The first correction maintains the short-term synchronization. The second correction is necessary to keep the synchronization from drifting off on a long-term basis.

The range scan memory is capable of holding two complete range scan patterns. When one range scan pattern is complete the radar hardware automatically starts working on the next one. As soon as the data from the just completed scan pattern is processed, the following scan pattern with the associated time wasting legs is transferred to the range scan memory FIFO. Since that transfer must be made before the radar hardware finishes processing the scan pattern it is presently working on, there is a lag built into the tracking loop.

VII. Range Tracking

The 51 elevations are averaged for each angular scan of the beam. If the mean elevation is not at the horizontal reference level of the range scan pattern, the next scan pattern transferred to the radar is shifted up or down accordingly. Because of the lag built into the tracking loop the next range scan pattern is only shifted by half the observed difference. Fig. 12 shows how the tracker would respond to a step function in mean elevation. If the shift had been equal to the observed difference the loop would have oscillated and not recovered. It should be emphasized that the tracker simply positions the center of the range scan pattern and has nothing to do with the elevation computation. As long as the target lies anywhere within the range scan pattern the correct elevation will be computed.

VIII. Scan Automatic Gain Control

The digitally programmable attenuators in the second IF system are used to compensate for the average variation in the return signal during each antenna scan. If the aircraft were in a 15° bank, the decrease in the mean signal power could be large as the incidence angle varied from 0° to 28°. Two effects would contribute to the decrease. The first is the falloff of radar cross section with increasing angle off-nadir. This falloff [3]–[5] is present for both sea, where it is windspeed dependent, and land, where it is terrain dependent.

The second cause of the power falloff is the range spreading effect illustrated in Fig. 13. When the beam is directed at nadir the surface within the beam will generally lie within one range cell and all the power is reflected at one time. But when the beam is off-nadir the surface within the beam is generally spread over a number of range cells and the returned power is divided into several ranges with a resulting decrease in peak power compared to the nadir case. The range spreading effect increases with aircraft altitude.

During the startup portion of the computer program,

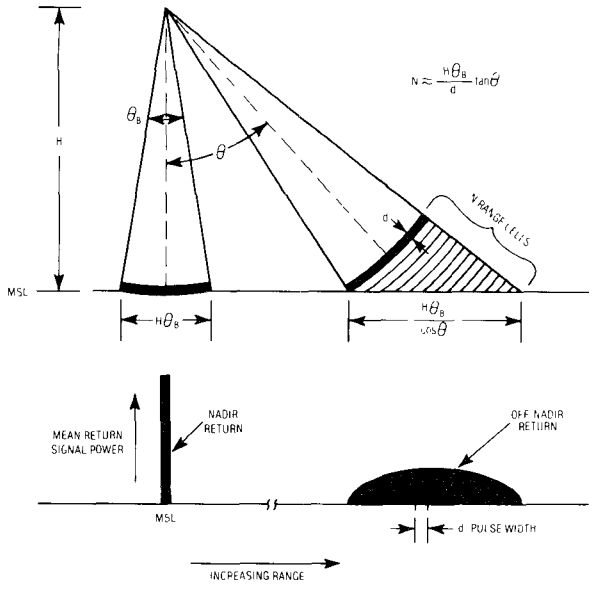

Fig. 13. Off-nadir the return power can be spread over a significantly greater range than at nadir with a resulting lower peak value.

falloff variations are computed for combinations of any of six different wind speeds with any of five different range spreading effects. While the radar is taking data the operator can select any of the five range spreading characteristics based on the aircraft altitude. At the operator's option, the wind speed characteristic can be selected either manually or by the computer based on the observed variation of mean returned power with incidence angle. When the computer selects the AGC array, the operator can select the averaging time used in the determination. Each data transfer from the computer to the radar hardware contains information to set a value on the programmable attenuators for each of the legs of the range scan pattern according to the aircraft roll angle and the selected wind speed and range spreading effects.

IX. Startup and Code Alignment

At the beginning of the startup phase the computer program displays questions on the CRT terminal about critical operational parameters such as the date, the aircraft nominal altitude, the largest vertical extent of the target expected within the swath, and the desired radar range resolution. When all the parameters have been inserted via the keyboard, the computer determines a nominal angular scan rate for the oscillating mirror and adjusts the drive motor speed accordingly. If a nonzero response was made by the operator when the vertical extent was requested, the angular speed is determined so that the radar range will step through twice that distance in the time it takes the beam to swing from 0.3° on one side of nadir to 0.3° on the other side. That allows the sensing of an elevation discontinuity in either direction equal to the vertical extent specified. If the operator responds to the vertical extent query with zero, then the computer reads the aircraft ground speed from the INS and determines the mirror angular frequency to provide an along-track overlap of 50 percent for the 3-dB footprint at nadir. After allowing time for transients to die out the actual angular scan period (as an integer multiple of Δt) is measured by observing the shaft angle encoder over approximately 10 s. Then the range scan patterns and other supporting quantities are computed.

Before the radar command to begin processing data is initiated, two range scan arrays are computed and shifted into the range scan memory FIFO. The 13 time wasting legs on the first array are designed to waste time with no net change in range. The 51 data legs are all 41 units long and the range increments on all of them. They result in an advance in range of 2091 units. The 13 time wasters of the second array are designed to back up in range by 2071 units. The 51 data legs of the second array also all advance and are 41 units long. The results of the second array are computed and displayed but not used. The second array is just to keep the hardware busy while computations are performed on the results of the first array to generate the third array. At the end of the second array the range is 2111 units from the starting point of the first array.

Once those two arrays are in the FIFO, alignment of the phases of the transmitter and receiver code modulators to obtain a zero-range reference can begin. The radar RF signal is directed via a waveguide switch and directional coupler into the receiver demodulator instead of the transmitter TWT amplifier and the command to start using the data in the range scan memory FIFO is initiated. From that point on, the computations are real-time and the range scan memory FIFO is never allowed to empty before the next scan pattern is transferred into it.

When the first scan pattern is complete, the ISP values from the first 50 data legs (whose total range change of 2050 units spans the pseudo-random modulation code length) are examined to determine which interval has the peak power. The reference for zero radar range (where the transmitter and receiver codes are aligned in the calibration configuration) should be KBAR, the centroid of the return power within that leg. To be certain that the zero-range reference was not thrown off by noise, a third alignment array is calculated whose 51 data legs are each only 9 units long. To make it easier for the operator to determine that a proper alignment has been carried out, the time wasters are used to position the starting point of the 51 advancing data legs so that the position of the peak observed in the first alignment array will occur at the fifth (middle) of the 9 steps of the twenty-sixth (middle) of the 51 data range scan legs. The fourth array is the same as the third but with the starting point shifted by 4 steps. It is used to occupy the radar hardware while the final zero-range reference is computed from the third array.

X. Target Acquisition

Having established a zero-range reference the next step is acquiring the target. While the shaft angle encoder is monitored over several cycles, range scan arrays are generated which result in no net range change but bring the range scan pattern into synchronization with the oscillat-

ing mirror. The signal path is then switched to the transmitter tube. To eliminate the need to consider changes in the surface scattering characteristics with angle and geometrical corrections for changing range to altitude, target acquisition data is acquired only within $\pm 2.5°$ of nadir. The range search advances through the entire code length using data range scan legs of 57 unit length. It takes 36 legs to cover the 2047 code length, 18 legs for the 1023 code and 9 legs for the 511 code. In general, it will require several antenna scans to complete the process, depending on the antenna oscillating mirror speed and the code length. The rest of the 51 data range scan legs are used simply as additional time wasters with no net range change so that the desired advancing legs that fall within the $\pm 2.5°$ limitation about nadir are contiguous in range from one antenna scan to the next.

Since the radar hardware can only determine range modulo the code length, the nominal altitude specified must be correct to within one half the code length or 152 m (381 m in the case of the 10-ns resolution) for the true absolute altitude to be determined. Operationally this presents no problem since the aircraft barometric altimeter is much more accurate than that. Roll information from the INS is used in the computation of the time wasting scans to synchronize the range search with nadir-pointing of the beam and to select the proper scan pattern once acquisition has occurred. Target interception is detected by searching for the range scan leg with the largest total return power and the centroid of the power within that leg is used to determine the range modulo the code length. The appropriate number of code lengths are added to result in an absolute range that is closest to the nominal altitude. Appropriate time wasters are computed to shift the range to the starting range and they and the appropriate steady-state range scan pattern are loaded into the range scan memory FIFO to begin steady-state operation.

XI. Supporting Features

In order to monitor the effect of the AGC patterns, an "A" scope displays the video signals during the range scans. To make it easier to interpret the display, it is also possible to unblank the scope only at one of five selectable antenna scan angles (nominally $0°, \pm 7°, \pm 13°$) and the video for the next range scan segment is displayed. The program also presents in real time on segmented displays the nominal altitude and the actual altitude as calculated from the radar data.

The system utilizes a graphic display unit driving a color TV monitor to display the falsely color-coded elevations in real-time. Sixteen system color bar configurations of 60 elements each are available and may be selected in real time by the operator using switches in the S register of the computer.

XII. Asymmetry in the Elevation Scan Rate

Although the range scan rate ($\Delta r/\Delta t$) is constant in magnitude for a given range resolution, the rate of change of the elevation interrogated $\Delta h/\Delta t$ is not. It is given by the expression

$$\frac{\Delta h}{\Delta t} = -\frac{\Delta r}{\Delta t}\cos\theta + r\frac{\Delta \theta}{\Delta t}\sin\theta. \tag{1}$$

The first term on the right is the range rate made negative and modified by the cosine of the angle of incidence θ to obtain the vertical component. The second term accounts for the decrease in the elevation interrogated at constant range when the antenna beam is swung towards nadir and vice versa. The first term reverses itself on each range scan leg but the second term does not and produces an asymmetry for the vertical rate of adjacent legs.

If the computer adjusts the antenna scan rate for a 50-percent overlap of the illuminated spot at nadir from one antenna scan line to the next, then the asymmetry is independent of aircraft altitude (for a constant aircraft ground speed). Under those conditions and for a ground speed of 70 m/s, the second term in (1) is approximately 0.4 percent of the magnitude of the first near nadir. At 14.7° off-nadir it is between 7 and 17 percent, depending on the scan pattern, and at 28° off-nadir it is about 22 percent.

The asymmetry effect must be considered in the development of the range scan patterns but it does not result in any error in the elevation measurements. Since adjacent range scan legs interrogate approximately the same vertical extent, an asymmetry in vertical rate results in a different number of steps on adjacent legs and an asymmetry in the horizontal distance moved by the beam during adjacent range scan legs. When the range scan patterns are generated during the startup phase of the computer program the legs are computed in pairs starting from nadir. The total horizontal distance moved by the beam during each pair of legs is set equal to the distance subtended by 1.2° at nadir. The number of steps is then distributed between the two legs so that the mean of the starting elevation of the first leg and the ending elevation of the second leg is as far above (or below) the horizontal reference level of the pattern as the starting elevation of the second leg is below (or above).

XIII. Asymmetry in the Antenna Scan Pattern

It is not possible for the type of mechanical linkage which drives the oscillating mirror to produce true sinusoidal motion. But because the rotating arm is short (2.1 cm) compared to the connecting link (21.6 cm), which is nearly perpendicular to the lever arm (7.7 cm) on the mirror shaft, the motion is approximately sinusoidal. The maximum deviation of the pointing of the beam from that of a true sinusoid of the same amplitude is about 0.6°. The angular variation is also asymmetrical, leading a sinusoid going in one direction and lagging it going in the other direction. A sinusoid is the best compromise between the two.

For each of the 51 range scan patterns the computer must store the 51 leg lengths, and the 52 ranges and 52 cosine complements at the beginning and end of the legs. The computer also needs the oscillating mirror shaft angle encoder value to be expected at the end of the scan, the

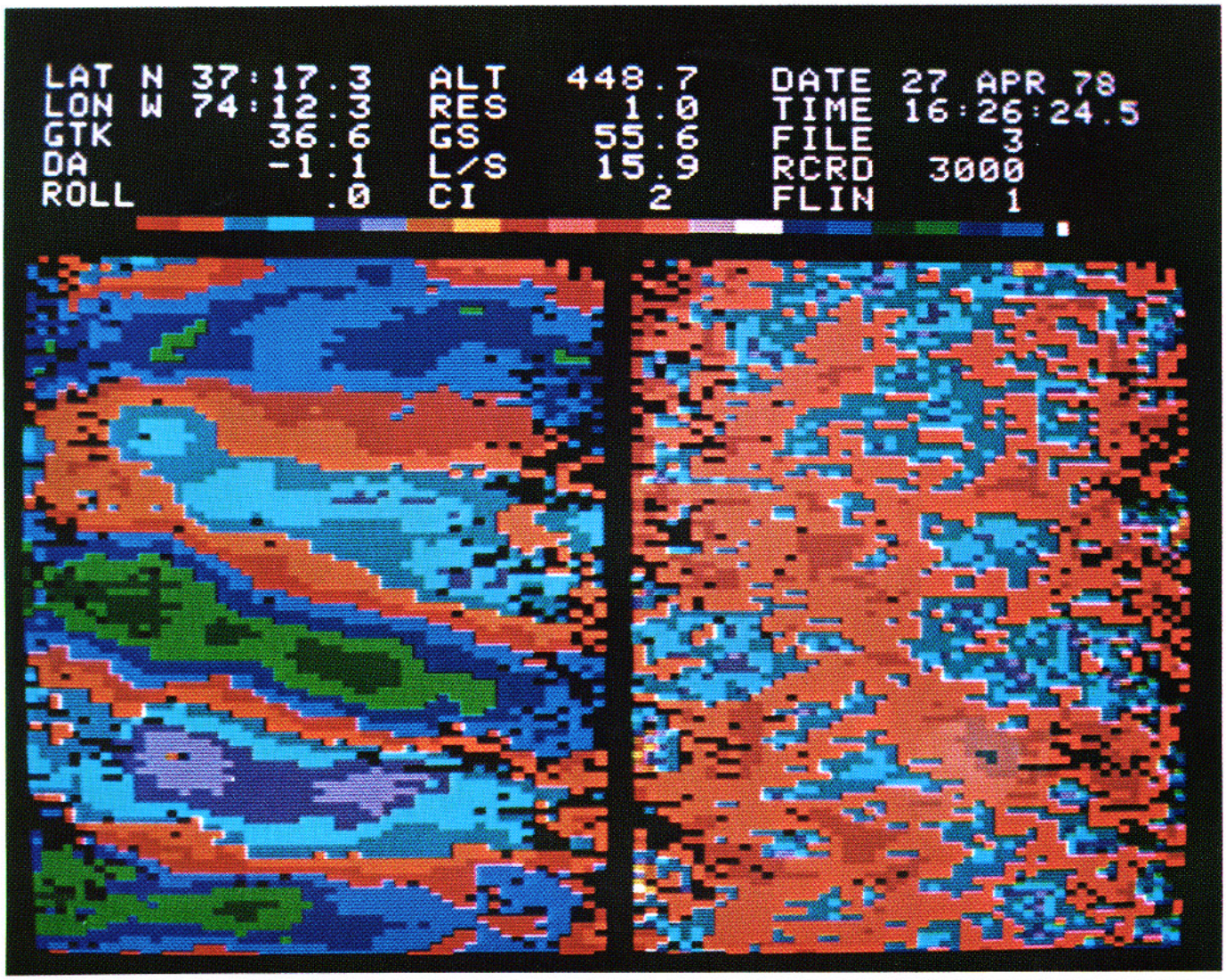

Fig. 14. SCR display for a 5.5-m SWH with the aircraft flying into the wind. On the left, each color indicates a 0.9-m change in surface elevation and on the right each color represents a backscattered power change of 50 percent of the mean power at that angle off-nadir.

nominal time from the end of the data portion of the range scan pattern to the reversal point of the mirror, and the nominal time from the mirror reversal point to the beginning of the data portion. That is a total of 7956 numbers and there was not sufficient memory left in the 32K computer to double it. The scan patterns were computed assuming the scan was sinusoidal.

The differences between the actual angular variation and the assumed sinusoid result in elevation biases which need correction. But even if those differences were eliminated by using the actual angular variation in computing the cosine complements, there would still be angular errors if the motor speed varied slightly so the period differed from the nominal value. A simple bias correction is generated which eliminates most of the bias in the real-time display. It uses two 51 element arrays (one for scanning left to right and one for right to left) to average a large number of elevation data points using an exponential weighting. During post-flight processing, biases are calculated for each scan pattern and for each value of angular error at the end of the range scan pattern from the average of a large quantity of data over water.

XIV. Observation Results

Fig. 14 is a photograph of the color TV monitor displaying data for a 5.5-m SWH sea with the aircraft flying perpendicular to the wave crests. The left side of the display is the elevation map with each color change representing an elevation change of 0.9 m. The data have been bias corrected and an exponential smoothing has been applied cross-track and along-track with the weighting decaying by half with each step. The aircraft was in level flight as indicated by the 0° aircraft roll angle (ROLL) shown at the top of the display. The nominal stable flight air speed of the aircraft is approximately 75 m/s. The aircraft 55.6 m/s ground speed (GS) and 1.1° drift angle (DA), which is the difference between the aircraft heading and the 36.6° aircraft ground track (GTK), show that the aircraft was headed very nearly into the wind. There are 100 scan lines displayed with the top line being the most recent and the bottom line being the oldest. The wind direction at the 448.7-m aircraft altitude (ALT) was somewhat different than the surface wind and the waves are propagating from the top right to the bottom left of the display.

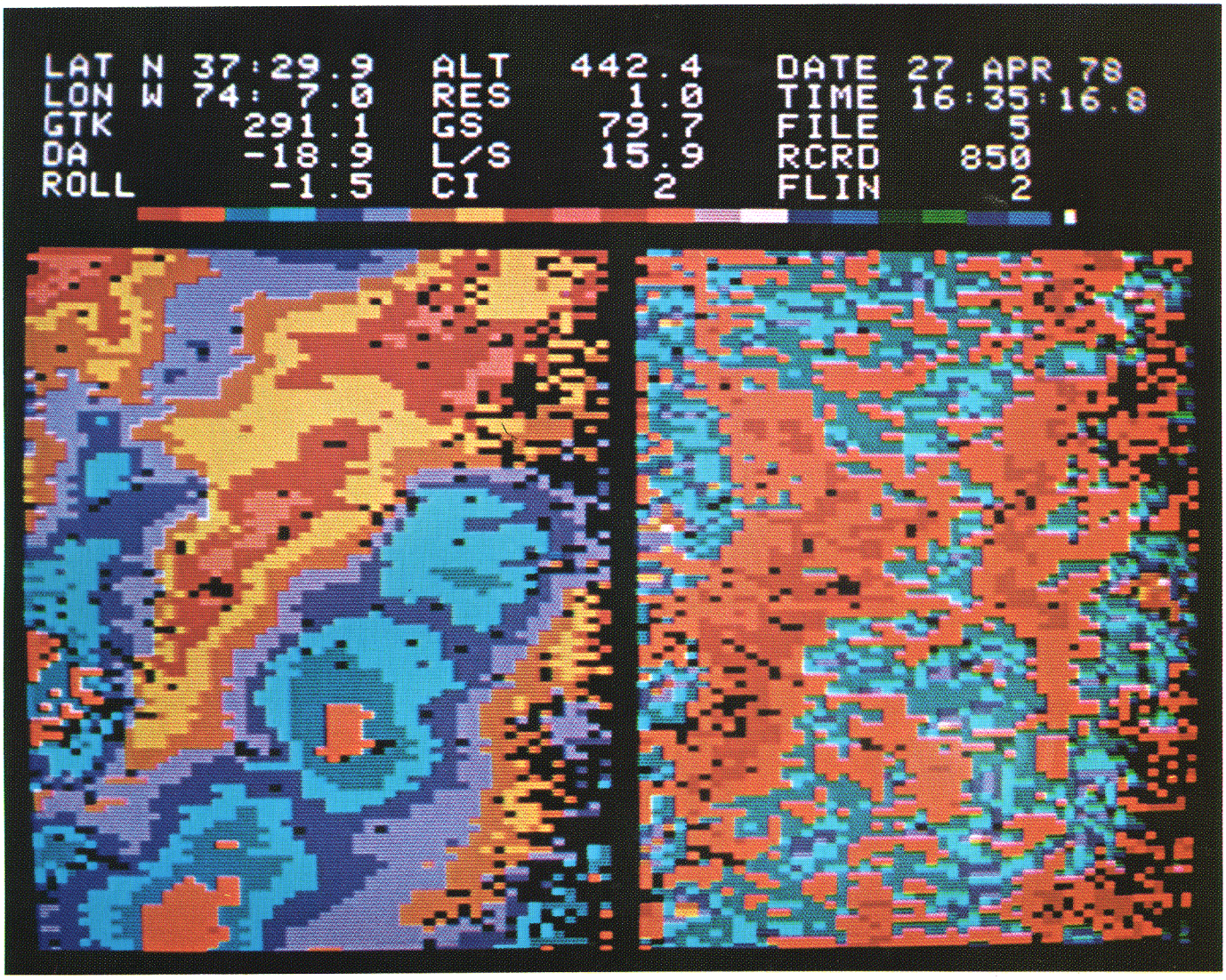

Fig. 15. Same conditions as for Fig. 14 but with aircraft flying perpendicular to the wind.

The range resolution (RES) used in acquiring the data was 1 ns. There are 60 elements in the color bar at the top of the figure. For Fig. 14, each color in the color bar is 3 range cell units wide (0.45 m) and a contour interval (CI) of 2 has been assigned. Therefore, a change in color represents an elevation change of 6 range cell units (0.9 m). The colors are in pairs to make it easier to determine the gradient visually. A change from light to dark of the same color denotes a decrease in elevation. The elevation information is permitted to wrap around in the color bar. In the lower half of the picture there is a dark green trough on each side of a light purple crest. By counting the color changes it can be seen that the crest to trough elevation change of the wave was approximately 9 m.

The antenna was scanning at 7.95 Hz or 15.9 lines per second (L/s). So the 100 line display represents approximately 6 s of data and contains 5100 data points. The black areas represent data dropouts, return signals that were too weak to process. The cross track dimension is approximately 224 m, half the aircraft altitude. The 350 m along track surface dimension for the data displayed can be arrived at by multiplying the time interval by the ground speed. There are approximately 2.5 wavelengths contained in the figure so the dominant wavelength is approximately 140 m and the ratio of wavelength to SWH is 25.4. Forecasts had predicted surface winds of 30 knots with gusts to 45 knots and the wind had been blowing in excess of 30 h. Most of the data on April 27 was taken in a torrential rainstorm.

The right side of Fig. 14 shows the relative radar backscattered power normalized within each off-nadir angle interval. The same along-track and cross-track exponential filter used for the elevations has been applied to the normalized power. The color-coding order starts at the left in the color bar. Deep orange represents a return signal power that is less than 50 percent of the mean power returned at that angle off-nadir. Light orange represents a return signal power between 50 and 100 percent of the mean power returned at that angle off-nadir. Each succeeding color represents an additional increment of the return signal equal to 50 percent of the mean power at that angle off-nadir.

Fig. 15 shows a segment of data on the same day flying crosswind. The aircraft was aligned crosswind by maximizing the drift angle. The crests and troughs appear to

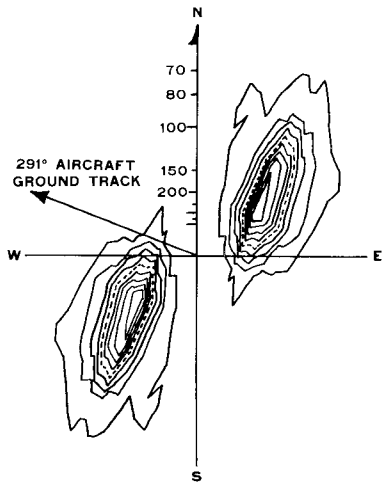

Fig. 16. Directional wave spectrum corresponding to flight path of Fig. 14. Contour interval is 10 percent of spectral peak with 50-percent contour dashed.

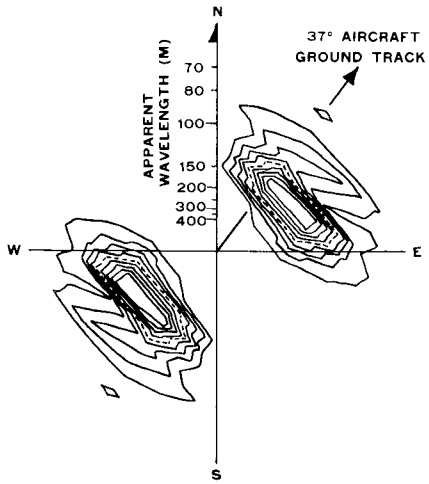

Fig. 17. Directional wave spectrum corresponding to flight path of Fig. 15.

orient themselves from top right to bottom left, instead of the naturally expected top to bottom. This resulted from a combination of effects: 1) the wind direction changed with altitude, and 2) the large drift angle of the aircraft (−18.9) meant that the beam was not scanned perpendicular to the aircraft's ground track. The phase velocity of the ocean waves was approximately 14 m/s. The wind velocity at the aircraft altitude was approximately 10 m/s higher than that. So the waves would seem to drift to the right relative to the aircraft, although they were actually propagating towards the left. The apparent angle is exaggerated by a 20-percent compression in the vertical dimension of the display relative to the horizontal dimension for the particular set of parameters in Fig. 15.

Figs. 16 and 17 show the directional spectra contours for the two different flight paths. Fig. 16 displays the wave height spectrum contours for the upwind flight path while Fig. 17 represents the crosswind flight conditions. The spectra are the averages of two-dimensional FFT's applied to each of twelve consecutive groups of 256 data lines of 51 elevation points. The spectra have been normalized

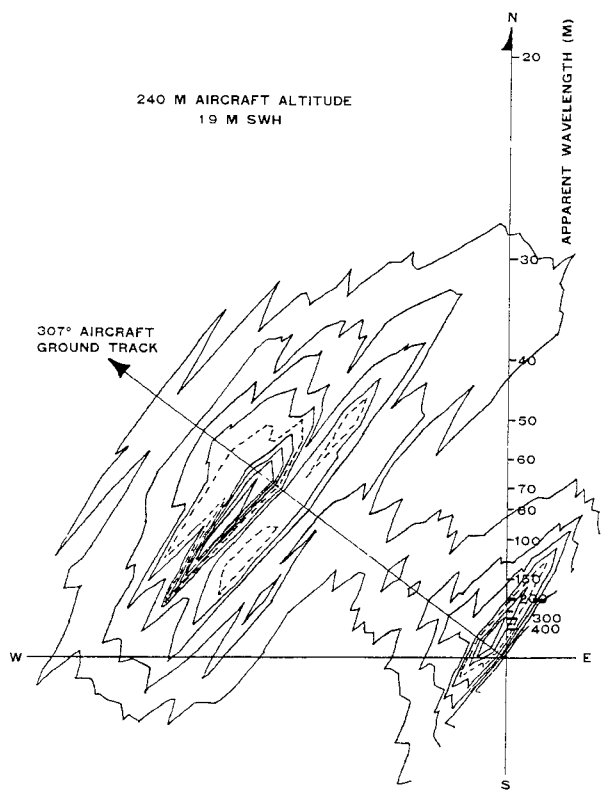

Fig. 18. Directional wave spectrum for 1.9-m SWH condition generated by a northwest wind.

with the contours representing 10-percent intervals relative to the spectral peak. The dashed contour represents the 50-percent power level. In each of the figures the mirror image of the spectra is also displayed. The spectra in the two figures were calculated from data taken at an aircraft altitude that resulted in a cross track swath width of approximately 1.6 ocean wavelengths rather than the desired seven wavelengths indicated in Fig. 1. The resulting blossoming of the spectra in the cross track direction due to the narrow swath is apparent. However, even when operational constraints mandate such a situation, it is apparent that obtaining information in orthogonal directions can greatly improve the determination of directionality.

Fig. 18 shows the directional spectra for a 1.9-m SWH condition when the flight path was nearly perpendicular to the crests of waves generated by a northwest wind. Only the mirror image of the spectrum is shown so the aircraft flight direction could be indicated while keeping the figure size reasonable. Along with the 41-m wavelength energy, there is also a swell whose apparent wavelength is nearly 400 m. The flight log indicated that there was a swell visible coming from the southeast.

The apparent wavelengths of the waves will be distorted by the normal Doppler effects due to the wave velocity relative to the aircraft velocity. The wavelengths of waves traveling in the opposite direction as the aircraft will appear shortened and those of waves traveling in the same direction will appear lengthened. The effect is more pronounced for longer wavelengths since their phase velocity

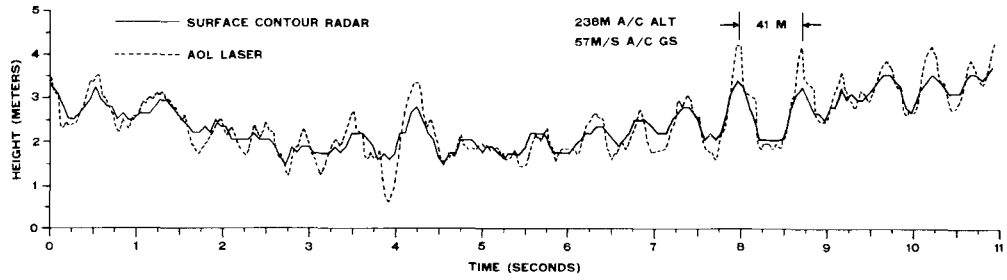

Fig. 19. Comparison of center swath elevation data from SCR and a profiling AOL laser system.

is higher. This effect is calculable and correctable but it has not been removed from these spectra.

A slice of data taken out of the center of the swath of the radar is compared with a profile taken by the NASA Airborne Oceanographic Lidar (AOL) laser system [1] in Fig. 19. The AOL, which was also developed under the NASA AAFE program, is installed in the same aircraft and the two profiles are time coincident. The laser had a spot size of $\sim 1/6$ m, while the SCR spot size was 3.4 m. The laser data was taken at 200 pulses per second and filtered using an 11 point sliding average. The general trend in the data is caused by aircraft motion. The disparity between the data sets in some of the wave amplitudes is caused by two effects. First, the SCR spot size causes some spatial filtering which tends to reduce the apparent wave amplitudes. Second, the AOL is subject to a threshold gating effect which tends to enhance the apparent wave amplitudes. Techniques to compensate for these effects are under study.

XV. Discussion and Conclusions

The purpose of this paper was to describe the SCR and outline its measurement capabilities. It is apparent that the system is capable of producing a real-time topographic map of the sea surface which was only previously available through photography and laborious stero reduction techniques [2].

An important oceanographic aspect of the SCR in contrast to the Synthetic Aperture Radar (SAR) is that the SCR produces surface elevation data through direct range measurements. The SAR measurement is indirect in that it is essentially a microwave photograph of the sea surface. The sea-state conditions are inferred from the intensity of the reflected radiation but the backscattering mechanisms are still not completely understood. Since the SCR simultaneously acquires both elevation and intensity information it should be invaluable in evaluating and more completely understanding the interpretation of SAR information. It is also planned to use the SCR for terrain mapping.

XVI. Acknowledgment

The authors would like to express their thanks an gratitude to many people who were instrumental in th development of the system. At NRL: B. S. Yaplee cor ceived the original idea for the instrument; J. W. Titu and W. L. Krewson designed the oscillating mirror; R. C Wilkinson assisted with the data electronics design; D. I Hammond had helpful suggestions in smoothing out de sign concepts. At WFC: D. C. Young designed the trans mitter pod; P. R. Evans and J. Hand assisted in th aircraft installation; D. E. Hines maintains and modifie the hardware; D. W. Hancock maintains and modifies th software; P. Bradfield and R. L. Navarro assisted in fligh scheduling support. K. Fisher of Ideas, Inc. did the earl software development. To G. L. Donner of Gary Donne Associates we owe a special thanks for his development c the real-time software and the sophisticated system fc editing and retrieving information from the magnetic tap and computer memory. The development effort woul have been severely hampered had it not been for hi dedication and resourcefulness. And last, but not least, T. McGoogan of WFC is thanked for his patience durin the debugging period.

References

[1] C. Bressel, I. Itzkan, J. E. Nunes, and F. E. Hoge, "Airborn oceanographic Lidar system," in *Proc. 11th Int. Symp. Remo Sensing of the Environment* (Environmental Research Institute Michigan, Ann Arbor, 1977), vol. 2, pp. 1259–1268, 1977.

[2] L. J. Cote, J. O. Davis, W. Marks, R. J. McGough, E. Mehr, W. Pierson, J. F. Ropek, G. Stephenson, and R. C. Vetter, "Th directional spectrum of a wind generated sea as determined fro data obtained by the stereo wave observation project," *Meteoro Papers* (Col. Eng., New York Univ., New York), vol. 2, no. 6, 196

[3] C. R. Grant and B. S. Yaplee, "Backscattering from water and lan at centimeter and millimeter wavelengths," *Proc. IRE*, vol. 45, pp 972–982, July 1957.

[4] W. L. Jones, L. C. Schroeder, and J. L. Mitchell, "Aircraft measur ments of the microwave scattering signature of the ocean," *IEE Trans. Antennas Propagat.*, vol. AP-25, pp. 52–61, Jan. 1977.

[5] L. S. Miller, "Investigation of the applications of GEOS-3 rad data in remote sensing of land and sea features," NASA Contract Report CR-141428, Aug. 1977.

[6] M. I. Skolnik, *Radar Handbook*. New York: McGraw-Hill, 197 ch. 20, p. 20.